communications materials

ARTICLE

https://doi.org/10.1038/s43246-023-00365-4 OPEN

Additive manufacturing of a high-performance aluminum alloy from cold mechanically derived non-spherical powder

J. Hunter Martin[1]✉, John E. Barnes[2,3], Kirk A. Rogers[3], Jacob Hundley[1], Darby L. LaPlant[1], Siavash Ghanbari[4], Jung-Ting Tsai[5,6] & David F. Bahr[4]

Metal additive manufacturing provides a path to optimized component design with significant realized advantages in the medical and aerospace industries. Limitations to expansion to other industries, e.g. automotive, and to enabling supply chain relief is the limited number of materials available and the ability to produce material on demand. Current additive manufacturing powder feedstock is produced at large, remote atomization facilities with long lead times. Here we identify a new "on-demand" powder production technology, cold mechanically derived, able to produce non-spherical powder for additive manufacturing, with high efficiency, and wrought equivalent material properties. We analyze the powder flow characteristics and mechanical properties comparing typical gas atomized with the new process demonstrating wrought property equivalence despite power sourcing. This research will enable expansion of additional alloy systems as well as encourage the processing of non-spherical powders to expand the available supply base of new alloys for additive manufacturing.

[1] HRL Laboratories LLC, Malibu, CA 90265, USA. [2] Metal Powder Works, Clinton, PA 15026, USA. [3] The Barnes Global Advisors LLC, Sewickley, PA 15143, USA. [4] School of Materials Engineering, Purdue University, West Lafayette, IN 47907, USA. [5] Argonne National Laboratory, Lamont, IL 60439, USA. [6] Present address: National Taiwan University of Science and Technology, Taipei 10607, Taiwan. ✉email: Jhmartin@hrl.com

Metal additive manufacturing (AM) is a rapidly growing field with initial applications focusing areas such as medical and aerospace, with high performance requirements[1,2]. AM has also found a niche solving supply chain issues with the greater use of local, distributed manufacturing[3]. This "on demand", highly customizable fabrication offers a future opportunity for local manufacturing bases to quickly tackle supply chain constraints or repair critical equipment. However, today there are only a limited selection of metal alloys available as a AM appropriate powder adding complexity to convert the part to be processed in AM but change the material as well[4,5]. Accomplishing this requires both available equipment and available raw material. The latter is the largest long term constraint due to the energy required, non-local nature of the current manufacturing strategy, and limited available materials[6].

Highly spherical gas and plasma atomized (GA and PA respectively) powders are the primary sources for metal additive manufacturing (AM) with anticipated exponential growth in the next decade[1,3,4,7]. In these atomization processes the material is heated to the melting point and a nozzle of flowing gas or plasma breaks the liquid metal into fine particles which form spheres due to surface tension as they fall and cool through an atomization chamber[8]. Powder production technologies like PA and GA have advanced rapidly with multiple processes now available, while simultaneously consolidating to a few suppliers due to the complexity and hazards associated with metal powder production[7,9]. Meeting the growing demand of the additive industry and expanding to additional communities is commiserate with a robust supply chain of quality feedstock. Here we demonstrate that with appropriate processing conditions non-spherical powders can be successfully utilized in AM, producing structures with the equivalent properties of high strength wrought materials while substantially increasing the availability of raw materials.

The GA process is estimated to use up to 11.5 kWh/kg (42 MJ/kg) for aluminum powder production, equating to ~5 kg of CO2/kg of aluminum produced[6,10]. Typical AM powder yields can be <20–40% depending on design of gas dies (e.g. free-fall and close-coupled) where over and undersized particles are discarded, increasing total energy use for AM powder to > 50kWh/kg and CO2 emissions >25 kg of CO2/kg of usable AM aluminum powder[4,6,10]. 95% of this carbon footprint of GA is due to gas use during atomization[6]. Decreasing emissions from source material, increasing availability of metal AM feedstock, and enabling end of life reuse of scrap material requires both a new powder production technique as well as industry equivalent metallurgical and mechanical performance of the AM product.

AM has been identified as a key tool for future advanced manufacturing due to the ability to topologically optimize components and near on-demand fabrication of components increasing component performance and reducing lead time, but only if feedstock material is reliably available[1,2]. AM technologies like Powder Bed Fusion (PBF), Binder Jetting (BJ), Directed Energy Deposition (DED), and Cold Spray (CS) all use metallic powder as a feedstock and are currently reliant on GA and PA powder supply chains[1,3,11]. A new, direct low energy, solid state production process for powdered feedstock termed cold mechanically derived (CMD) powder production has been developed to enable local on-demand fabrication of additive feedstock, but lacks the spherical nature of typical GA and PA powders (Fig. 1)[12]. Local production of powdered metal from industrially available stock (e.g. rod, machining chips, wire) or direct recycling of metallic components offers several advantages including reduced lead times, reduced onsite powder storage, increased availability of new alloys, reduced waste, and improved industrial hygiene by limiting personal contact with metallic powder[9]. Limited studies on alternative methods to GA have been investigated utilizing non-spherical powder but have been limited to hydride-dehydride material (e.g. Ti6Al4V) or focused on DED of machined chips[13–15]. In the former this limits the applicable material to hydride forming materials, and in both sieving, sizing, and waste is generated.

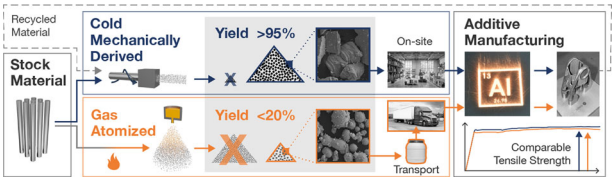

Fig. 1 Powder processing approaches. Cold mechanically derived powder provides a lower energy, distributed production methodology with >95% yield over conventional gas atomized powder while providing equivalent material properties.

Al7075 remains one of the most used alloys in aerospace and high performance applications both for future development and sustainment of existing infrastructure and vehicles[16–18]. Al7075 powder was procured in two forms GA and CMD powder. Powder compositions were within typical Al7075 specification[19] although each differed slightly (Supplementary Table 1). CMD powder was produced for this study using a novel low carbon emission, gas free process developed by Metal Powder Works. The process rotates a bar a a prescribed RPM with a specially design tool impacting the bar along its length. The tool has multiple teeth and upon impact, each tooth generates a particle of a target size range dictated by the parameter inputs. The frequency of impact is controlled such that millions of particles are generated each second with high repeatability in size resulting in metallic particles of a very specific target particle size distribution (PSD) with yields of >95%[12]. Due to the mechanical nature of the particle formation, iron was measured in the powder composition as a surrogate for cutting tool contamination and found to be well within material tolerance (Supplementary Table 1). Energy use is on the order of 3.4kWh/kg, measured via probe during processing, providing a low energy input suitable for local renewable energy powered processing (e.g. solar). The room temperature processing associated with this approach enables additional opportunities for onsite powder production distributing the energy burden related to maintaining stock material and decreasing the long range delivery of powdered metals typically requiring ground transportation due to material hazards[9].

Here we present an alternate, low energy consumption feedstock source that can produce material locally with wrought equivalent properties in a high strength aluminum alloy. This overcomes several current limitations in powder sourcing while providing high performance materials "on demand."

Results and discussion

Powder characterization. The Al7075 alloy, like the most 7000 and 2000 series alloys are not considered weldable and therefore not readily usable in fusion based AM processes[20]. These alloys are the highest strength aluminum alloys and are commonplace in aerospace and other high performance industries[16]. These high value alloys are not readily usable in AM due to solidification cracking related to the microstructure and solute rejection[20]. In this study, CMD and GA powders were each rendered "printable" in AM via a functionalization process described by Martin et. al. but first demonstrated here on non-atomized material[20]. Each material was then characterized for flow characteristics and finally processed into mechanical test components via laser powder bed fusion (L-PBF). Mechanical properties were then measured and compared to each other, common AM Al alloys, and typical

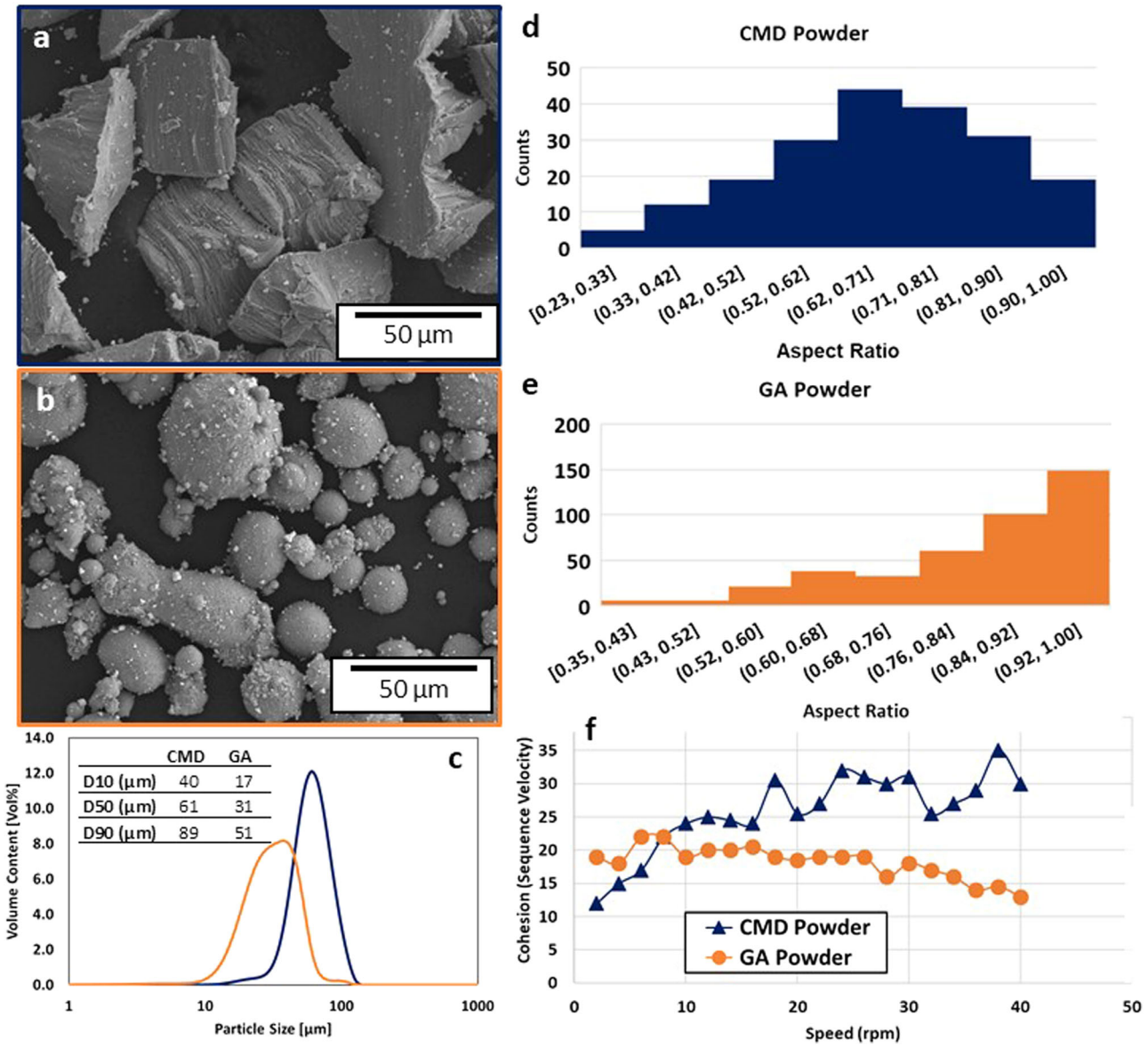

Fig. 2 Assessment of powder characteristics. a SEM image of functionalized CMD powder, **b** SEM image of functionalized GA powder, **c** Powder size distribution of CMD and GA powder, **d** aspect ratio of CMD powder, **e** aspect ratio of GA powder, **f** Cohesive index vs rotation speed for CMD and GA powder. Additional data in Supplementary Figs. 2–4.

wrought alloy properties to evaluate the overall impact of powder production and morphology on performance.

AM powder use has trended towards highly spherical powder morphologies with specific particle size distributions to ensure predictable flow and spreading during recoating between layers and high packing density to ensure melt-pool continuity during processing[21]. The true requirements for fully dense fabrication and powder characteristics have not been fully evaluated, however enabling high aspect ratio and lower packing density would enable a broader selection of powder production processes. The CMD process produces an equiaxed with a sphericity of 0.8 to 0.85 (Fig. 2a, b), which could be increased to a sphericity of >0.9 with spheroidization. Subsequent spheroidization technologies do exist, they rely on inert gas flow which increases the carbon footprint and cost of production[22].

In order to understand the applicability of CMD material for AM it is firstly important to understand the characteristics of the powder when compared to industry standard GA powder. Functionalized powder was first quantifiably characterized for morphology (Fig. 2d, e). While GA powder does trend toward a spherical nature, it does deviate slightly from perfectly spherical due to the formation of satellites (redeposited material during the atomization process) as well as oblong powders developed due to stochastic instability events during fluid break up during atomization and inability to spheroidize during the liquidus dwell time[4]. Conversely CMD powder contains faceted particles with higher aspect ratios consistent with the mechanical forming technique. Particle size distribution also indicates noticeable differences, (Fig. 2c). The GA powder analyzed in Fig. 2 has been sieved and sorted to meet the industry standard AM cut of powder with a broad peak to increase packing density. CMD powder was produced with a slightly larger average particle size and tighter distribution but no sieving and sizing was completed enabling >95% powder yield from input feedstock vs <20% typical of GA powder[4].

The combined effects of powder morphology and particle size distribution are major factors in the ability for a granular media to flow[23]. The Hausner ratio is a metric comparing tap density to “fluff” density and related to the compressibility index,

$CI\% = 100 \times \frac{V_0 - V_f}{V_0}$. While the tap density of the CMD powder (53%) is lower than GA powder (59%), the "fluff" density is also lower providing Hausner ratios of 1.15 and 1.24 for GA and CMD powder respectively, where ratios <1.25 are typical of materials with qualitatively good flow[23]. While important for several material handling steps in AM, the ability to recoat and deposit smooth layers in a powder bed is important.

Granudrum experiments, where powder is photographed and analyzed in a rotating clear drum, were conducted to understand the cohesive index and angle of repose (Fig. 2f)[24]. At low RPMs, consistent with low recoater speeds typical in current commercial AM systems, CMD and GA powders show very little difference. At increased speeds, CMD powder begins to deviate from GA resulting in a shear thickening effect, likely due to increased non-spherical powder interactions and indicative of material binding increasing the angle of repose.

A critical cohesive index of 25 and tap densities of >45% were anticipated to be required for high quality recoating and meltpool continuity respectively as supported by several previous studies[24–27]. Both GA and CMD powders meet these criteria and should therefore be equally suitable for AM. CMD powder likely requires a tighter coater speed window during handling due to the shear thickening behavior and a lower recoat speed to ensure low cohesion.

Material processing. After analyzing the powder behavior a strategy for processing both powder types in L-PBF was developed to account for the varying flow behavior however all coating and air flow parameters were within normal operating conditions for both materials. A layer thickness of 45 µm was chosen for the CMD powder to account for the PSD and lower packing factor compared to 30 µm for the GA powder. A brief parameter study was conducted varying laser power, speed, and hatch spacing resulting in as-built densities of 2.77 g/cc and 2.79 g/cc for CMD and GA powder respectively. Final selected processing parameters used are in Supplementary Table 2.

Resulting as-built microstructures of GA and CMD materials were consistent with functionalized high strength aluminum including highly refined crack free microstructures (Fig. 3)[20]. A bimodal distribution of grain sizes is seen with columnar grains at the melt-pool boundary and are hypothesized to nucleate off the available Al_3Zr in the previous layer and propagate quickly in the high thermal gradient at the meltpool boundary during the incubation time of new Al_3Zr inoculants[20]. After the initial columnar growth thermal gradients towards the meltpool center have decreased and solidification rate increases with a high density of Al3Zr inoculant phases resulting in a distribution of small (>10 µm) equiaxed grains[28]. Maintaining the refined microstructure is critical to avoiding solidification cracking[20].

Grain size in AM Al7075 materials is about 10X smaller than typical grains in wrought Al7075[29]. Reduced grain size is not anticipated to have an appreciable impact on strength due to the low hall-petch coefficient in aluminum, however small grains may provide additional benefits including enhanced fatigue life and crack growth resistance[30,31]. Furthermore addition of Zr has been shown to improve corrosion resistance, which is a common problem in many high strength aluminum alloys[32].

Material characterization. Previous attempts at AM of 7000 series processing resulted in significant vaporization of Mg and Zn with gravimetric losses of 35% and 25% respectively[20]. Vaporization of zinc and magnesium was also observed in this study, however the overall magnitude was reduced due to lower incident laser energy density and further refinement of parameter sets for high strength Al alloys. CMD powder showed the least vaporization with 12% Mg and 25% Zn loss with GA powder showing 26% Mg and 31% Zn loss (full as printed compositions in Supplementary Table 3). Increased vaporization of high vapor pressure elements in the GA powder is likely due to the lower volumetric energy density used for CMD powder processing. Since Zn and Mg are key strengthening elements this would be anticipated to lower overall material strength, however higher retention than previous studies should result in improved mechanical properties. In both GA and CMD material, as-built composition retains lower than specified Al7075 Zn content, while only GA material is low on Mg content due to vaporization during processing.

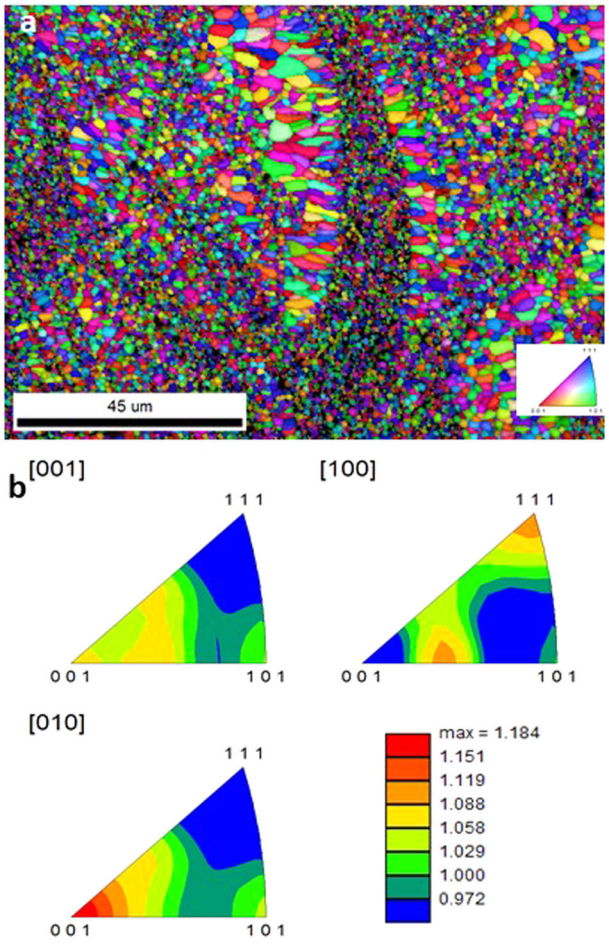

Fig. 3 Microstructure characterization of CMD L-PBF material. a EBSD microstructure indicating a bimodal grain size distribution with refined grains at melt-pool boundaries and elongated grains near the melt-pool center. **b** Inverse pole figures are different reference orientations indicating relatively random orientations due to the small range of the color map.

Extruded tensile ASTM E8 Type II style tensile specimens were printed from GA and CMD powders to evaluate the mechanical performance of components produced from each material and compare against wrought Al7075 alloy stock (Supplementary Fig. 1). Microscopy evaluation of parts produced from both CMD and GA powders indicated relative densities of 98.6% and 99.3% respectively in the as-built state. This indicates that further refinement of parameter sets is possible, but outside the scope of this study. To separate the influence of residual porosity from that of the powder processing method, specimens produced from each type of powder were evaluated after heat treatment of the as-built condition and with the inclusion of a hot isostatic pressing (HIP) step to close porosity and provide an indication of inherent material properties devoid of critical flaws. HIP was completed at 400 °C to reduce the chance of incipient melting and 207 MPa to ensure material flow for 2 hours. After HIP both materials were measured at 2.81 g/cc, the anticipated

theoretical density. Aging heat treatments were consistent with industry T6 standards with a solution treatment at 480 °C for 1 h followed by a room temperature water quench and aging at 121 °C for 13 h and air cooled.

After heat treatment, tensile specimens were machined to match ASTM E8 Type II final dimensions using a non-contact wire EDM. Tensile testing was conducted in accordance with ASTM E8 and the mechanical properties for both the HIP and heat treat conditions of parts produced from GA and CMD powder is shown in Fig. 4 and Table 1. Data in the Table 1 is the average of >6 coupons and subsequent standard deviation [full data in Supplementary Tables 4 and 5]. Representative tensile curves for the three materials of interest are shown. The associated results indicate all materials processed are roughly equivalent to the wrought Al7075 T6 alloy. CMD powder showed slightly higher strength and ductility than both GA powder and wrought 7075 demonstrating excellent promise for target applications.

Focus is given to the HIP'd coupons as they are assumed to be more indicative of inherent material properties rather than those associated with AM processing, which is anticipated to improve with further parameter refinement. It is however important to understand the differences. The most notable difference in the HIP'd coupons is the substantial increase in ductility along with statistically significant increases in yield strength. Residual porosity in the non-HIP'd coupons is driving early failure and decreasing the cross-sectional load bearing capacity. This is further illuminated in the associated deviation in elastic modulus

Both HIP'd and non-HIP'd CMD material shows improved strength and ductility over GA, however material superiority over GA and wrought material is unclear due to varying processing parameters. Increased vaporization of the strengthening elements in GA material likely decreased the strength, while additional changes in Zn/Mg/Cu ratios in the alloy could impact the final liquid composition during solidification leading to a higher tendency for brittle grain boundary phase formation such as S-phase[33,34]. Further parameter optimization and process control will be important for all AM processing of materials with high vapor pressure elemental additions.

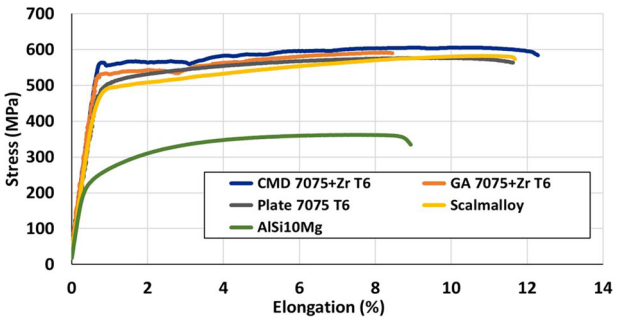

Fig. 4 Tensile response of GA and CMD material. Representative tensile curves of GA and CMD materials and relevant comparisons to plate 7075-T6, AlSi10Mg, and Scalmalloy.

Conclusion

A mechanical property equivalency to wrought Al7075 with both CMD and GA powder and AM processing has been established. GA and other atomization technologies reliant on flow instability of liquid metal for powder production are inherently infrastructure intensive and therefore require non-local fabrication to support an increasingly distributed additive supply base. Furthermore these approaches can be >3X more carbon intensive with >4X lower yields due to the high energy density required in the production of inert gasses unless gas recovery and recycling or a shift to renewable energy gas production are implemented[6]. Non-spherical powders require more controlled AM processing due to changes in flow character, however these changes are manageable within the current industrial equipment. Eliminating the requirement of atomization substantially increases the availability and diversity of metal feedstock while reducing the carbon footprint of powder production for AM with no apparent impact on static material properties.

Enabling powders not limited to production by GA or PA will enable greater material availability as well as adoption of additional non-spherical production methodologies readily available in industry water atomization, Hydride-DeHydride (HDH) and spray drying. High yield production methods decrease the affordability barrier for new materials increasing research level availability. Mechanical processing produces highly consistent and repeatable lots providing a more feedstock more amenable to lower variability end products. The solid state conversion of material feedstock also improves quality through chemical consistency avoiding volatilization of high vapor pressure elements during liquid state processing. Distributed, on-demand, low energy production, also opens the door to metal AM in remote or contested environments where powder shipments would be difficult or too costly, but local scrap material could be converted to AM feedstock for fabrication of community critical infrastructure.

Materials and methods

Powder production. CMD powder was produced by Metal Powder Works from wrought 7075 rod stock and provided to HRL in an as produced state. GA powder was procured from Valimet in the requested 7075 composition. Both materials were functionalized in accordance with Martin et al. [20] utilizing electro static assembly via powder blending and used in the as functionalized state. Care was taken to avoid moisture and oxygen contamination in compliance with standard industrial powder handling.

Powder analysis. Powder size, distribution, and shape were measured using a Malvern Morphology G3-ID particles shape analyzer. A small volume of metallic powders was dispersed on the flat transparent substrate with air pressure. Each sampling analysis was performed for more than 4000 particles. The imaging system utilized automatic static imaging to measure the size and shape distribution of powders. The measuring range was 1 μm to 1000 μm. The particle size parameters such as circular equivalent diameter, length, width, aspect ratio were measured in this analysis. The powder morphology was documented using scanning electronic microscopy (SEM, FEI Corp., Quanta, USA). Powder particles were placed on

Table 1 Overview of mechanical properties with average and standard deviation observed in CMD and GA materials as well as typically observed values in plate 7075-T6[35], Scalmalloy[36,37], and AlSi10Mg[38] as well as previous efforts to print crack free 7075[20].

Material	Modulus (GPa)	Yield strength (MPa)	UTS (MPa)	Elongation (%)
CMD 7075+Zr T6	71.9 ± 1.5	543.3 ± 19.1	597.4 ± 11.1	12.1 ± 2.3
GA 7075+Zr T6	72.4 ± 1.3	527.4 ± 5.5	587.4 ± 6.8	8.4 ± 0.8
Plate Al7075 T6[35]	71.7	372–469	462–538	11.6
AM Al7075[20]	63–66	325–373	383–417	3.8–5.4
Scalmalloy[36,37]	70–72	475–490	520–580	10–14
AlSi10Mg[38]	69–70	200–215	300–370	7–10

carbon tape attached to an aluminum disc before each analysis to ensure the particles are fully conductive but not charged.

The angle of repose measurement was conducted using a rotating drum (GRANUDRUM). The experimental rotating drum was a horizontal cylinder with glass sidewalls and with a capacity of $1000cm^3$. The rotating drum was filled with metallic powders to approximately 55% of volume capacity. The angle of repose measurement was captured using a fluorescent backlight over angular velocities with 2 rpm increments applied from 0 to 40 rpm. For each velocity measurement, 50 images with 0.5 s intervals have been taken to record the images. Finally, the position of the powders and empty space in the drum is determined by edge detection. Following sequences during drum rotation were observed in the slope of the powders and air interface inside of the drum chamber. At a lower speed of the drum, metal powders moved with the drum speed until the dynamic repose angle reach the maximum angle, after this point and increasing the angle small avalanches were created. With increasing the rotating speed, powders move down due to the avalanche formation. Further increasing the rotating speed causes the slope angle to approach a steady-state situation.

The tapped density and Hausner ratio were determined using a GranuPack instrument Powders are fed to the measurement cell. The instrument tapped the powder cell with 1 mm fall taps. After each tap, the measurement of powder height was performed by an inductive sensor. By using the height and weight of the powders in the cell, tapped densities were determined.

Printing. All GA and CMD powder was printed in a Renishaw 500Q system utilizing the Renishaw reduced build volume insert. This uses a double piston system at a 1:1 feed ratio and a slightly larger feed container. A standard rubber coating blade was used. Components were designed in Solidworks then loaded into the Renishaw QuantAM software along with build parameters. Printing was conducted under flowing industrial argon. Initial parameter development was completed on 1 cm^3 blocks. After printing, powder was removed and components were sonicated in water.

Printed material analysis. During parameter development 1cm3 blocks were tested for density using helium pycnometry with an AccuPyc II 1340 series He pycnometer system. Cross-sections were made of dense specimens for SEM/EBDS and prepared using industry standard metallographic techniques. EBSD was conducted by EBDS analytical and data was provided for interpretation. HIP was conducted at AIP (American Isostatic Presses). Heat treatments were conducted in lab air. Quenching was conducted within 15 s of removal from the furnace in >10 gal of water. Parts were immediately removed from the quench bath and placed in a separate aging furnace. Machining of final tensile geometries was conducted using industry standard machining practices. Tensile testing was conducting in accordance with ASTM E8 on and Instron 5500 Universal Testing System with a 50 kN load cell. A coupled full field digital image correlation using an ARAMIS 4 M system was used to determine elongation, yield strength, and ultimate tensile strength. Bars of AlSi10Mg and Scalmalloy of the same geometry were procured from Protolabs and 3D Alchemy respectively and tested in the same method to obtain curves for Fig. 4.

Data availability

The datasets generated during and/or analysed during the current study are available from the corresponding author on reasonable request.

Received: 12 December 2022; Accepted: 11 May 2023;
Published online: 27 May 2023

References

1. Frazier, W. E. Metal additive manufacturing: A review. *J. Mater. Eng. Perform.* **23**, 1917–1928 (2014).
2. Das, S., Bourell, D. L. & Babu, S. S. Metallic materials for 3D printing. *MRS Bull.* **41**, 729–741 (2016).
3. Howard, D. State of the P/M industry - North America. *Powder Metall. Int.* **57**, 31–34 (2021).
4. Anderson, I. E., White, E. M. H. & Dehoff, R. Feedstock powder processing research needs for additive manufacturing development. *Curr. Opin. Solid State Mater. Sci.* **22**, 8–15 (2018).
5. Anderson, I. E. & Terpstra, R. L. Progress toward gas atomization processing with increased uniformity and control. *Mater. Sci. Eng. A* **326**, 101–109 (2002).
6. Dopler, M. & Weiß, C. Energy consumption in metal powder production. *BHM Berg- und Hüttenmänn. Monatsh.* **166**, 2–8 (2021).
7. Whohlers Report 2022. *Whohlers Report 2022: 3D Printing and Additive Manufacturing State of the Industry, Annual Worldwide Progress Report* (Wohlers Associates, 2022).
8. Lagutkin, S., Achelis, L., Sheikhaliev, S., Uhlenwinkel, V. & Srivastava, V. Atomization process for metal powder. *Mater. Sci. Eng. A* **383**, 1–6 (2004).
9. Maynard, E. & Pittenger, B. H. *Additive Manufacturing Processes* (ASM International, 2020).
10. EPA. *AVERT, U.S. National Weighted Average CO2 Marginal Emission Rate, Year 2019 Data*. (2020).
11. Najmon, J. C., Raeisi, S. & Tovar, A. Review of additive manufacturing technologies and applications in the aerospace industry. *Addit. Manuf. Aerosp. Ind.* https://doi.org/10.1016/B978-0-12-814062-8.00002-9 (2019).
12. Barnes, J. & Aldridge, C. System and method for the manufacture of ductile material powder. US Patent Application US20210146442A1 (Filed 04-04-2019).
13. Jackson, M., Deshpande, A., Kim, A. & Pfefferkorn, F. A study of particle size metrics using non-spherical feedstock for metal additive manufacturing. *Proc. Manuf.* **53**, 519–524 (2021).
14. Jackson, M. A., Kim, A., Manders, J. A., Thoma, D. J. & Pfefferkorn, F. E. Production of mechanically-generated 316L stainless steel feedstock and its performance in directed energy deposition processing as compared to gas-atomized powder. *CIRP J. Manuf. Sci. Technol.* **31**, 233–243 (2020).
15. Wu, Z. et al. Study of printability and porosity formation in laser powder bed fusion built hydride-dehydride (HDH) Ti-6Al-4V. *Addit. Manuf.* **47**, 102323 (2021).
16. Starke, E. A. & Staley, J. T. Application of modern aluminum alloys to aircraft. *Prog. Aerosp. Sci.* **32**, 131–172 (1996).
17. Immarigeon, J. P. et al. Lightweight materials for aircraft applications. *Mater. Charact.* **35**, 41–67 (1995).
18. Miller, W. et al. Recent development in aluminium alloys for the automotive industry. *Mater. Sci. Eng. A* **280**, 37–49 (2000).
19. Society of Automotive Engineers. & American Society for Testing and Materials. *Metals and Alloys in the Unified Numbering System (UNS)*. (ASTM International, 2012).
20. Martin, J. H. et al. 3D printing of high-strength aluminium alloys. *Nature* **549**, 365–369 (2017).
21. Fedina, T., Sundqvist, J. & Kaplan, A. F. H. The use of non-spherical powder particles in Laser Powder Bed Fusion. *IOP Conf. Ser. Mater. Sci. Eng.* **1135**, 012018 (2021).
22. Bao, Q., Yang, Y., Wen, X., Guo, L. & Guo, Z. The preparation of spherical metal powders using the high-temperature remelting spheroidization technology. *Mater. Des.* **199**, 109382 (2021).
23. Geldart, D., Harnby, N. & Wong, A. C. Fluidization of cohesive powders. *Powder Technol.* **37**, 25–37 (1984).
24. Shanbhag, G. & Vlasea, M. Powder reuse cycles in electron beam powder bed fusion— variation of powder characteristics. *Materials (Basel).* **14**, 4602 (2021).
25. Le, T. P., Wang, X., Davidson, K. P., Fronda, J. E. & Seita, M. Experimental analysis of powder layer quality as a function of feedstock and recoating strategies. *Addit. Manuf.* **39**, 101890 (2021).
26. Körner, C., Bauereiß, A. & Attar, E. Fundamental consolidation mechanisms during selective beam melting of powders. *Model. Simul. Mater. Sci. Eng.* **21**, https://doi.org/10.1088/0965-0393/21/8/085011 (2013).
27. Le, K. Q., Tang, C. & Wong, C. H. A study on the influence of powder packing density on the melt track in the selective laser melting process. *Proc. Int. Conf. Prog. Addit. Manuf.* **2018-May**, 703–708 (2018).
28. Martin, J. H. et al. Grain refinement mechanisms in additively manufactured nano-functionalized aluminum. *Acta Mater.* **200**, 1022–1037 (2020).
29. Waldman, J., Sulinski, H. & Markus, H. Effect of ingot processing treatments on the grain size and properties of Al alloy 7075. *Met. Trans.* **5**, 573–584 (1974).
30. Thangaraju, S., Heilmaier, M., Murty, B. S. & Vadlamani, S. S. On the estimation of true hall-petch constants and their role on the superposition law exponent in Al alloys. *Adv. Eng. Mater.* **14**, 892–897 (2012).
31. Hahn, G. T. & Rosenfield, A. R. Metallurgical factors affecting fracture toughness of aluminum alloys. *Metall. Trans. A* **6**, 653–668 (1975).
32. Kim, Y. S. et al. Investigation of Zirconium effect on the corrosion resistance of aluminum alloy using electrochemical methods and numerical simulation in an acidified synthetic sea salt solution. *Materials (Basel).* **11**, 1982 (2018).
33. Yu, J. & Li, X. Modelling of the precipitated phases and properties of Al-Zn-Mg-Cu alloys. *J. Phase Equilibria Diffus.* **32**, 350–360 (2011).
34. Marlaud, T., Deschamps, A., Bley, F., Lefebvre, W. & Baroux, B. Influence of alloy composition and heat treatment on precipitate composition in Al–Zn–Mg–Cu alloys. *Acta Mater.* **58**, 248–260 (2010).
35. Boyer, H. E. & Gail, T. L. *Materials Handbook Desk Edition* (ASM International, 1985).
36. AP Works. *Material Data Sheet- Scalmalloy. ScAlmAlloy Material Data Sheet* http://www.sigmaaldrich.com/catalog/product/aldrich/541443?lang=en&region=IL (2016).
37. Schmidtke, K., Palm, F., Hawkins, A. & Emmelmann, C. Process and mechanical properties: applicability of a scandium modified Al-alloy for laser additive manufacturing. *Phys. Proc.* **12**, 369–374 (2011).
38. Lewandowski, J. J. & Seifi, M. Metal additive manufacturing: a review of mechanical properties. *Annu. Rev. Mater. Res.* **46**, 151–186 (2016).

Acknowledgements
The authors wish to acknowledge the internal funding from HRL which enabled this work to be completed as well as the help of John Carpenter in crafting the figures. The authors also thank Metal Powder Works for providing materials to conduct the experiments presented here.

Author contributions
J.H.M., J.E.B., K.A.R., J.H., and D.F.B. conceived of, lead the research efforts, and drafted the manuscript, J.E.B. and K.A.R. provided CMD powder and guidance on handling. J.H. and D.L.L. functionalized and printed the CMD and GA powder. D.L.L. completed tensile tests, S.G., J.T.T., and D.F.B. conducted powder analysis and characterization. J.H.M., J.E.B., K.A.R., and D.F.B. reviewed and compiled data. All authors reviewed and provided feedback on the manuscript.

Competing interests
The authors declare no competing interests.

Additional information
Supplementary information The online version contains supplementary material available at https://doi.org/10.1038/s43246-023-00365-4.

Correspondence and requests for materials should be addressed to J. Hunter Martin.

Peer review information *Communications Materials* thanks Amir Mostafaei and the other, anonymous, reviewer(s) for their contribution to the peer review of this work. Primary Handling Editors: Cang Zhao & John Plummer.

Reprints and permission information is available at http://www.nature.com/reprints

Publisher's note Springer Nature remains neutral with regard to jurisdictional claims in published maps and institutional affiliations.

Open Access This article is licensed under a Creative Commons Attribution 4.0 International License, which permits use, sharing, adaptation, distribution and reproduction in any medium or format, as long as you give appropriate credit to the original author(s) and the source, provide a link to the Creative Commons license, and indicate if changes were made. The images or other third party material in this article are included in the article's Creative Commons license, unless indicated otherwise in a credit line to the material. If material is not included in the article's Creative Commons license and your intended use is not permitted by statutory regulation or exceeds the permitted use, you will need to obtain permission directly from the copyright holder. To view a copy of this license, visit http://creativecommons.org/licenses/by/4.0/.

© The Author(s) 2023